Resting-state Functional Connectivity of the Right Temporoparietal Junction Relates to Belief Updating and Reorienting during Spatial Attention

Anne-Sophie Käsbauer[1], Paola Mengotti[1], Gereon R. Fink[1,2], and Simone Vossel[1,3]

Abstract

■ Although multiple studies characterized the resting-state functional connectivity (rsFC) of the right temporoparietal junction (rTPJ), little is known about the link between rTPJ rsFC and cognitive functions. Given a putative involvement of rTPJ in both reorienting of attention and the updating of probabilistic beliefs, this study characterized the relationship between rsFC of rTPJ with dorsal and ventral attention systems and these two cognitive processes. Twenty-three healthy young participants performed a modified location-cueing paradigm with true and false prior information about the percentage of cue validity to assess belief updating and attentional reorienting. Resting-state fMRI was recorded before and after the task. Seed-based correlation analysis was employed, and correlations of each behavioral parameter with rsFC before the task, as well as with changes in rsFC after the task, were assessed in an ROI-based approach. Weaker rsFC between rTPJ and right intraparietal sulcus before the task was associated with relatively faster updating of the belief that the cue will be valid after false prior information. Moreover, relatively faster belief updating, as well as faster reorienting, were related to an increase in the interhemispheric rsFC between rTPJ and left TPJ after the task. These findings are in line with task-based connectivity studies on related attentional functions and extend results from stroke patients demonstrating the importance of interhemispheric parietal interactions for behavioral performance. The present results not only highlight the essential role of parietal rsFC for attentional functions but also suggest that cognitive processing during a task changes connectivity patterns in a performance-dependent manner. ■

INTRODUCTION

The analysis of functional connectivity in resting-state fMRI time series has proven to be a useful approach to investigate the functional organization of the brain (Yeo et al., 2011). In resting-state functional connectivity (rsFC) studies, participants are not engaged in any particular task during data acquisition, and functional brain networks are revealed, for example, by analyzing spontaneously correlated low-frequency activity fluctuations across the brain (Biswal, Yetkin, Haughton, & Hyde, 1995). Regions forming a network at rest also show similar connectivity patterns during task-related activity (Hoffstaedter et al., 2014; Fox, Corbetta, Snyder, Vincent, & Raichle, 2006)—and these findings also relate to the structural connectivity of the respective brain regions (Greicius, Supekar, Menon, & Dougherty, 2009; Honey et al., 2009).

In the attention domain, regions that are coactivated in task-related fMRI studies show strong rsFC (Fox et al., 2006). More specifically, the dorsal and ventral attentional networks (Corbetta & Shulman, 2002) can be differentiated based on their resting-state connectivity patterns. Here, the temporoparietal junction (TPJ) is positively connected with the ventral attention network as well as the anterior insula, the dorsolateral pFC, and the midcingulate cortex (Bzdok et al., 2013; Kucyi, Hodaie, & Davis, 2012; Mars et al., 2012). Moreover, these connections are stronger for the right TPJ (rTPJ) than the left TPJ (lTPJ; Kucyi et al., 2012). Additionally, recent evidence suggests that anatomically and functionally distinct rTPJ subregions may exist (Bzdok et al., 2013; Mars et al., 2012). Strong rsFC was found between the lateral anterior pFC and a dorsal rTPJ cluster in the inferior parietal lobule. Conversely, an anterior ventral rTPJ subregion was more strongly connected to the ventral pFC and the anterior insula, and a posterior subregion showed stronger rsFC with the anterior medial pFC and a parietal network (Bzdok et al., 2013; Mars et al., 2012). Similar observations supporting the idea of functionally independent subregions in TPJ were also found for the lTPJ using a multivariate analysis of the BOLD signal (Silvetti et al., 2016).

The TPJ has been associated with a wide range of cognitive functions (see Igelström & Graziano, 2017, for a review), and it is still unclear whether this region mediates

[1]Institute of Neuroscience and Medicine (INM-3), Research Centre Juelich, [2]Faculty of Medicine and University Hospital Cologne, University of Cologne, [3]Faculty of Human Sciences, University of Cologne

a general cognitive process or whether it is involved in multiple domain-specific functions. Distinct subregions have been postulated to be associated with different functions, with the anterior region being linked to attention processes and the posterior region to social cognition (Krall et al., 2016; Bzdok et al., 2013). As a major node within the ventral attention network, the proposed primary attentional function of the rTPJ is reorienting attention toward unexpected stimuli, that is, acting as a "circuit breaker" for the dorsal top–down attention system consisting of the intraparietal sulci (IPS) and FEFs (Corbetta, Patel, & Shulman, 2008; Corbetta & Shulman, 2002). However, rTPJ has more recently also been associated with the more general function of "contextual updating" (Mengotti, Dombert, Fink, & Vossel, 2017; Vossel, Mathys, Stephan, & Friston, 2015; Geng & Vossel, 2013; Doricchi, Macci, Silvetti, & Macaluso, 2010), that is, the ability to update internal models of the current behavioral context for creating appropriate expectations and responses.

It remains to be investigated whether rTPJ subserves both reorienting and updating, respectively, and whether different rTPJ connectivity patterns underlie the two processes. Using modifications of the classical location-cueing paradigm (Posner, 1980), reorienting of visuospatial attention, and belief updating can be investigated within the same task. To this end, the percentage of cue validity (i.e., the proportion of valid and invalid trials) is manipulated throughout the experiment, and the participants have to infer the actual cue validity level (i.e., the probability that the cue will be valid in a given trial). Whereas reorienting is reflected in the RT difference between unexpected and expected target locations, belief updating is assessed by parameters of computational learning models based on single-trial RTs reflecting the adaptation of behavior to the inferred validity of the spatial cue (e.g., Mengotti et al., 2017; Vossel et al., 2014).

Although little is known about the link between TPJ rsFC and cognitive functions, first evidence for a significant relationship between rsFC networks and deficits in reorienting of attention has been provided by studies in stroke patients (Siegel et al., 2016; Corbetta et al., 2015; Baldassarre et al., 2014; Carter et al., 2010; He et al., 2007). For instance, impaired reorienting towards contralesional targets has been related to decreased interhemispheric rsFC of the IPS (Baldassarre et al., 2014; Carter et al., 2010; He et al., 2007) as well as decreased interhemispheric rsFC of the supramarginal gyri (He et al., 2007).

Given that the role of rsFC of rTPJ for the trial-wise updating of probabilistic beliefs has not yet been addressed and that rTPJ is putatively involved in both reorienting of attention and belief updating, this study aimed at characterizing the relationship between rsFC of rTPJ and these two cognitive processes. Task-based fMRI studies employing effective connectivity analyses have shown that connectivity changes between regions of the dorsal and ventral attention network are related to behavioral performance in spatial attention paradigms (Vossel et al., 2015; Vossel, Weidner, Driver, Friston, & Fink, 2012; Weissman & Prado, 2012; Wen, Yao, Liu, & Ding, 2012). Effective connectivity between lTPJ and rTPJ has been related to enhanced filtering of distractors (Vossel, Weidner, Moos, & Fink, 2016). Connectivity from rTPJ to the right IPS (rIPS) and from rTPJ to the right inferior frontal gyrus (rIFG) has been associated with reorienting of attention, especially when invalid targets are less expected (Vossel et al., 2012). Moreover, connectivity from rTPJ to FEF has been related to trial-wise belief updating about cue validity in a saccadic version of the location-cueing paradigm (Vossel et al., 2015).

In this study, we asked if reorienting and belief updating are related to rTPJ connectivity patterns at rest before the task—as well as to rsFC changes after the task. We chose an rTPJ seed linked to belief updating based on previous fMRI and TMS work (Mengotti et al., 2017; Vossel et al., 2015). In a first step, we characterized the rsFC pattern of this particular rTPJ region. In a second step, we correlated measures of belief updating and reorienting in a modified location-cueing task with rsFC of this area with dorsal and ventral network nodes before the task and with the rsFC changes from before to after the task. We predicted that the resting-state network architecture of rTPJ with the ventral and dorsal system would be related to behavioral performance, and we explored the specificity of the resulting associations for reorienting and belief updating, respectively.

METHODS

Participants

The study was approved by the ethics committee of the German Psychological Society, and written informed consent was obtained from all participants. All procedures in this study followed the Code of Ethics of the World Medical Association (Declaration of Helsinki).

For the resting-state measurements, we recruited 29 healthy volunteers with no history of neurological or psychiatric disorders. They had a normal or corrected-to-normal vision and were naïve to the purpose of the experiment. All participants were right-handed, as assessed with the Edinburgh Handedness Inventory (Oldfield, 1971).

After data acquisition, six participants had to be excluded from further analysis: one because of poor task performance (more than 2 *SD*s below the mean accuracy of all participants), one for a technical problem with the recording of the manual responses, and four because of excessive head movements (>1° in rotation parameters) during resting-state fMRI. Therefore, the final sample comprised 23 participants (14 women; age range = 20–36 years, mean age = 27 years).

Procedure

The data for this study were derived from a more comprehensive neurostimulation experiment, which consisted of

three sessions distributed over 3 days. According to a within-participant crossover design, each participant underwent two experimental sessions preceded by a preparation session. The data collected on the first day consisted of a high-resolution anatomical scan, preparatory measures for the neurostimulation, and practice of the experimental paradigm. In the second and third experimental sessions, active, continuous theta burst stimulation (cTBS) or "sham stimulation" was delivered (note that because of the use of a placebo [sham] coil, the sham stimulation did not involve any magnetic stimulation). In the sham session, the placebo coil was placed over the vertex. Each day started with a resting-state scan (~7 min duration), during which participants had no task apart from maintaining fixation on a central cross. Subsequently, the active motor threshold was determined to define the intensity of the stimulation, and the stimulation was delivered outside the scanner. After the stimulation (sham or active cTBS), the participant was transported to the scanner, and task-based fMRI (~23 min duration) as well as a second resting-state scan were performed. The task-based fMRI measurements started on average 5.37 min (SD = 43 sec) after the neurostimulation.

For our present research question on the role of rTPJ functional connectivity for belief updating and reorienting, we here exclusively focus on the resting-state scans and behavioral data from the task-based fMRI of the sham session of the study. Given that the sham session could be performed before or after the active cTBS session according to a crossover design, we tested for any session order effects in this data set (see below).

Paradigm during Task-based fMRI

We used a modified version of a location-cueing paradigm with central cueing (Posner, 1980) to assess attentional reorienting and belief updating about cue validity (%CV), as described in the study of Mengotti et al. (2017). Stimuli were presented on a 30-in. LCD screen behind the scanner at a distance of 245 cm. Participants saw the monitor via a movable mirror installed on top of the head coil. As a fixation point during the total duration of the task, a central diamond on a gray background was presented (see Figure 1A). In each trial, a spatial cue, consisting of an arrowhead pointing to either the left or right side, appeared for 400 msec to indicate in which hemifield the target would appear. After an 800 msec SOA, two diamonds appeared for 350 msec on the left and right side of the fixation point (5.8° eccentric in each visual field). The target was a diamond with a missing upper or lower corner. Participants had to press a button with the index or middle finger of their right hand to indicate which part of the target diamond (upper or lower corner) was missing. The response mapping was counterbalanced across participants. The intertrial interval was 2000 msec. During each experimental session, participants performed one run of eight blocks. Each block comprised 48 trials, resulting in 384 trials. The percentage of %CV, that is, the ratio of valid and invalid trials, was manipulated between blocks but was kept constant within each block. %CV within each block amounted to ~90% (87.5%), ~70% (71%), ~30% (29%), or ~10% (12.5%), respectively. In the 30% and 10% CV blocks, the cue was counterpredictive, as the majority of trials were invalid. At the beginning of each block, precise information about the %CV was given. However, in half of the blocks, the given information was false—resulting in misleading prior expectations. In these false blocks, the expected %CV was inverted concerning the true %CV. Participants were not instructed how many blocks were false and how distant the false %CV would be from the true one. They only knew that, in some blocks, false information could be given. Hence, the participants were instructed to use the spatial cues depending on how much they "trust" them and to estimate the true %CV. At the end of each block, participants had to explicitly state their estimated %CV using a 9-point

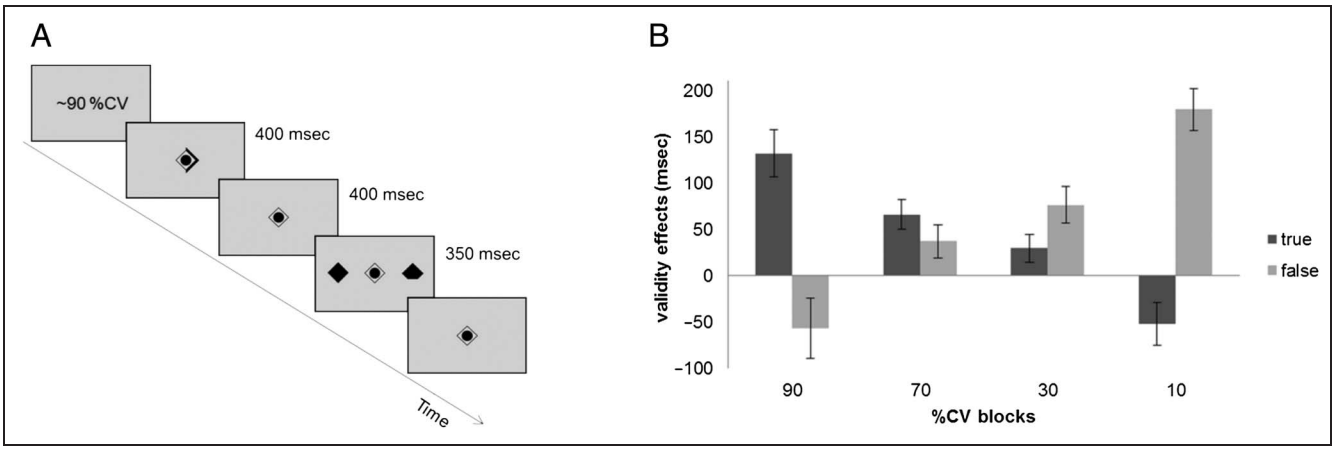

Figure 1. (A) Experimental paradigm with one example trial (valid trial). At the beginning of each block, the %CV (either true or false) was shown. This value was used as prior before the observation of the first trial in the modeling approach. On each trial, participants indicated whether the upper or lower corner of the target was missing. The participants were asked to maintain central fixation throughout the experiment. (B) VEs (RT invalid minus RT valid; mean ± SEM) for each true and false %CV block. The VEs vary linearly with actual %CV.

scale ranging from 10% to 90%, as well as the confidence in their rating. For the main trials, RTs and accuracy of the target discrimination were measured. Each participant completed a short practice before each experimental session consisting of two runs: One consisting of one block with a constant true 80%CV and the other comprising three blocks, with two blocks with true and one with false prior information about %CV.

Each participant was presented with the same sequence of trials within each block with two different block sequences for participants. Using constant trial sequences is a standard procedure in computational studies of learning processes that require inference on conditional probabilities in time series (e.g., Iglesias et al., 2013; Daunizeau et al., 2010). The duration of the paradigm was around 23 min.

Behavioral Data Analysis

Reorienting of Attention—Validity Effects

RTs were measured for each trial to allow an analysis of the behavioral data. Anticipations (RT < 100 msec), misses, and incorrect responses were excluded from the analyses, and mean RT was computed separately for valid and invalid trials.

The above-described paradigm requires the orientation of attention to the most likely target location. In valid trials with %CV > 50%, participants direct their attention covertly to the position indicated by the cue. The validity effect (VE) is the difference in RTs between invalid and valid trials and reflects the time necessary to reorient attention from an expected to an unexpected location (Posner, 1980). However, in the present paradigm, %CV was <50% in some blocks. In these counterpredictive blocks, the target was more likely to appear at the uncued location. To test whether the participants' behavior was affected by the different %CV levels (i.e., if they indeed inferred the actual %CV in the different blocks), the VE was calculated separately for each %CV block (see Figure 1B).

For the group-level analyses, averaged blockwise accuracy scores expressed in percentage of correct responses were used in a 2 × 2 within-participant ANOVA with the factors Prior (true, false) and Validity (valid, invalid). Because the manipulation of %CV was expected to mainly influence the speed of responding, mean RTs in each %CV block were subjected to a 2 × 4 × 2 within-participant ANOVA with the factors Prior (true, false), Block (90% CV, 70%CV, 30%CV, 10%CV), and Validity (valid, invalid). Because the blockwise VE was expected to vary linearly with the actual %CV, a subsequent 2 × 4 ANOVA on the VE (RT difference between invalid and valid trials) with the factors Prior (true, false) and Block (90%CV, 70%CV, 30% CV, 10%CV) was used. Here, we expected to find a significant linear trend for the Prior × Block interaction effect, because this would reflect the adaptation of behavior to %CV, that is, inference of the actual %CV levels by the participants. All group-level analyses were performed with SPSS (SPSS Statistics for Windows, Version 25.0, IBM). Results from these analyses are reported at a significance level of $p < .05$ after Greenhouse–Geisser correction where applicable.

To obtain an overall measure of reorienting speed for the correlation analyses with rTPJ rsFC (see below), the sign of the VE was inverted for counterpredictive blocks (where invalid trials were more frequent than valid trials), and the blockwise VEs were averaged. This measure should reflect the general magnitude of the reorienting costs at unexpected locations (i.e., target locations with an actual probability <50%, irrespective of the direction of the cue). To check for any session order effects, we conducted a two-sample t test on the mean VE between those participants who completed the sham before and after the cTBS session.

Belief Updating—Computational Modeling

A measure of belief updating about the actual validity of the spatial cue in this paradigm was derived from a computational learning model. For the modeling, single-trial RT was converted to response speed (RS = 1/RT) because RSs tend to be more normally distributed (Brodersen et al., 2008; Carpenter & Williams, 1995). To quantify belief updating about the %CV in true and false blocks, we applied a Rescorla Wagner (RW) model to trial-wise RSs in the different blocks. Because of the smaller number of trials entering the model and the block structure of the task with constant %CV in each block, a RW model, rather than a previously used hierarchical volatility-based Bayesian model (Vossel et al., 2014, 2015), was chosen, as in the study of Mengotti et al. (2017). It has been shown that the RW learning rate is significantly correlated with the Bayesian parameter describing the updating of %CV (Vossel et al., 2014). In both types of models, updating is influenced by the weighting of prediction errors (the discrepancy between observed and predicted outcomes) by a learning rate. Each block was modeled separately, and a higher learning rate was expected for false than true blocks.

In the RW model, updating of the belief that a cue will be valid in a single given trial equals the product of a learning rate α and the prediction error $\delta^{(t)}$, that is, the difference between the observed and the predicted outcome in the respective trial t. The updated prediction after experiencing the trial t, $P^{(t)}$, is then given by the sum of the prediction from the previous trial and the product of learning rate and prediction error.

$$P^{(t)} = P^{(t-1)} + \alpha\delta^{(t)}$$

Hence, the learning rate α determines the extent to which prediction errors influence the participant's belief from trial to trial. Considering that the learning rate α

affects the steepness of the exponential decay of the influence of preceding trials (Rushworth & Behrens, 2008), it also reveals to which extent past events change the participants' predictions. To estimate the RW learning rate α in each block, single-trial RSs were used. A linear relationship between $RS^{(t)}$ and the prediction before the observation of the outcome of the trial $P^{(t-1)}$ was assumed by the response model, which was employed to map from the participant's belief about %CV to observed responses (see Mengotti et al., 2017; Vossel et al., 2014, for a similar procedure).

$$RS^{(t)} = \begin{cases} \zeta_{1\_\text{valid}} + \zeta_2 P^{(t-1)} & \text{for valid trials} \\ \zeta_{1\_\text{invalid}} + \zeta_2\left(1-P^{(t-1)}\right) & \text{for invalid trials} \end{cases}$$

ζ_{1_valid}, ζ_{1_invalid}, and ζ_2 are additional participant-specific parameters that are estimated from the data. ζ_{1_valid} and ζ_{1_invalid} define the constants of the linear equation (i.e., the overall levels of RSs), and ζ_2 governs the slope of the affine function (i.e., the strength of the increase in RS with increased estimated %CV $P^{(t-1)}$). The learning rate α and the three parameters from the observation model were estimated from trial-wise RSs using variational Bayes as implemented in the HGF toolbox (www.translationalneuromodeling.org/tapas/) running on MATLAB (R2014a, The MathWorks, Inc.). Variational Bayes optimizes the (negative) free-energy F as a lower bound on the log evidence, such that maximizing F minimizes the Kullback-Leibler divergence between exact and approximate posterior distributions or, equivalently, the surprise about the inputs encountered (for details, see Friston, Mattout, Trujillo-Barreto, Ashburner, & Penny, 2007).

The learning rate α was averaged separately for the blocks with true and false prior information concerning %CV. As in our previous study (Mengotti et al., 2017), we expected a higher learning rate α in blocks with false prior information, because here contextual updating is required to estimate the true %CV. To test this assumption, a paired-sample t test on the learning rate α was calculated to compare blocks with true and false priors.

To obtain a measure of belief updating for the correlation analyses with rTPJ rsFC (see below), the difference in learning rates between false and true blocks was used. This difference score reflects the differential updating after false prior information has been provided. Additionally, to check for a session order effect, we conducted a two-sample t test on this difference score.

Resting-state fMRI Data Acquisition and Preprocessing

During the two resting-state measurements before and after task-based fMRI, participants had no task apart from maintaining fixation on a central cross. Using a 3T MRI System (Trio; Siemens), 180 T2*-weighted volumes were acquired applying an EPI sequence with BOLD contrast with a repetition time of 2.2 sec and an echo time of 30 msec. Each volume consisted of 36 axial slices with interleaved slice acquisition. The field of view was 200 mm, using a 64 × 64 image matrix, which resulted in a voxel size of 3.1 × 3.1 × 3.3 mm^3. The first five volumes were discarded from the analysis to allow for T1 equilibration effects. The remaining 175 volumes were analyzed using the Statistical Parametric Mapping software SPM12 (Wellcome Department of Imaging Neuroscience; Friston et al., 1995; www.fil.ion.ucl.ac.uk/spm) and FC toolbox CONN, Version 18.a (McGovern Institute for Brain Research, Massachusetts Institute of Technology; Whitfield-Gabrieli & Nieto-Castanon, 2012; www.nitrc.org/projects/conn). For the preprocessing, images were bias-corrected. Slice acquisition time differences were corrected using sinc interpolation to the middle slice. During spatial realignment, a mean EPI image was computed for each participant and spatially normalized to the MNI template using the segmentation function. Subsequently, the obtained transformation was applied to the individual EPI volumes to translate the images into standard MNI space and resample them into 2 × 2 × 2 mm^3 voxels. Finally, the normalized images were spatially smoothed using an 8-mm FWHM Gaussian kernel.

The pre- and posttask resting-state data were passed through several additional preprocessing steps using the CONN toolbox (Whitfield-Gabrieli & Nieto-Castanon, 2012) for MATLAB R2017b (The MathWorks, Inc.). Data were detrended and high-pass filtered (0.01 Hz). Head movement artifacts were removed with the artifact detection tools scrubbing procedure. White matter, cerebrospinal fluid, and movement parameters were extracted as nuisance covariates following the CompCor strategy (Behzadi, Restom, Liau, & Liu, 2007) and taken out by linear regression. Temporal derivatives of these confounds were also included in the linear model, accounting for time-shifted versions of spurious variance.

Seed-Based Functional Connectivity of rTPJ

rsFC was analyzed with seed-based correlation analysis. This method computes the temporal correlation between the BOLD activity from a given seed voxel to all other voxels in the brain using a general linear model approach (Fox et al., 2005; Biswal et al., 1995).

First, to identify areas showing positive or negative functional connectivity with the specific rTPJ region, a voxel-wise map was computed for the seed ROI, which was an 8-mm radius sphere centered at $x = 56$, $y = -44$, $z = 12$. This MNI coordinate was derived from a previous fMRI and TMS study investigating belief updating and reorienting (Mengotti et al., 2017; Vossel et al., 2015). The BOLD time series were averaged over all voxels in the seed ROI and the voxel-wise Pearson correlation coefficients between that ROI, and all other voxels were computed. After that, the Fisher z transformation was applied.

Participant-specific contrast images reflecting standardized correlation coefficients were used for the second-level random-effects analysis in SPM. We computed one-sample t tests to determine the main positive and negative rsFC maps of the rTPJ seed across pre- and posttask runs, respectively. To investigate differences in rsFC from pre- to posttask, we computed paired t tests. All results were thresholded at a voxel-wise $p < .05$ FWE-corrected with an extent threshold of ≥20 voxels. The locations of activation were derived from the Anatomy Toolbox for those regions that have been mapped cytoarchitectonically (Eickhoff et al., 2005). Additionally, to check for any session order effects, we conducted a within-participant ANOVA with the factors Session Order (active cTBS first, sham first) and Run (pretask, posttask) on the rsFC.

Brain–Behavior Relationship

To examine the relationship between pretask rsFC and the parameters of reorienting of attention and belief updating in the location-cueing task, we computed the Pearson correlation coefficient between each behavioral parameter (mean VE and the difference in learning rates α for false and true blocks) and the strength of rTPJ rsFC and six target ROIs. These six ROIs were chosen to comprise the critical regions of the dorsal and ventral attentional networks in both hemispheres (lIPS, rIPS, lFEF, rFEF, lTPJ, and rIFG). The coordinates of these ROIs were extracted from the local maxima in the respective anatomical areas in the main positive and negative rsFC maps of the rTPJ seed across pre- and posttask runs. The same analyses were performed using the differences in rTPJ connectivity from post- to pretask to investigate the relationship of the behavioral parameters with changes in rsFC after the task.

To check if outliers drove the correlations, we calculated Cook's distance (Cook, 1977). If Cook's distance values were >1 (Stevens, 1996) for a given participant, the correlations were recalculated without this participant to check if the significant relationship persisted.

As control analyses, we also performed the abovementioned analyses with more general task measurements, that is, overall RS and accuracy.

To investigate the specificity of our results for reorienting or belief updating, respectively, we used stepwise linear regression analysis with rsFC as dependent and the two behavioral parameters as independent predictor variables. This analysis determines the smallest set of predictor variables with the best model fit. The (minimum) corrected Akaike information criterion (AICC) was used to evaluate the effect of adding or removing the reorienting or belief updating parameter to/from the regression model. Here, it should be noted that both measures should be independent in the present paradigm, because we used a global measure for reorienting (averaged over all blocks with reversed signs for blocks with counterpredictive cues).

Eye Movement Recording

To verify that participants followed the instructions to maintain fixation, eye movements were monitored with an Eye-Link 1000 (SR Research) eye-tracking system with a sampling rate of 500 Hz during the practice session outside the scanner. At the start of the experiment, calibration and validation of the eye tracker were performed (validation error <1° of visual angle). Analysis of the data was performed using MATLAB (R2014a, The MathWorks, Inc.). The timing and stimulus configurations of the practice session were identical to the fMRI task. However, the targets were presented with an eccentricity of 8.9°. The critical period analyzed for gaze deviations from the center was the time window between the presentation of the cue and the target display (cue–target period). Saccades were identified as gaze deviations from fixation >1.5° visual angle in the cue–target period, and they were determined and expressed as a percentage score over the total number of trials. Three participants had to be excluded from this analysis because of the bad quality of the signal. Therefore, eye movement data from 20 of the 23 participants were analyzed.

RESULTS

Behavioral Results

Participants maintained fixation on average in 96% (*SEM* = 1.2%) of the trials. Overall, the average accuracy amounted to 95% (*SEM* = 1.56). The within-participant ANOVA on accuracy scores with the factors Prior (true, false) and Validity (valid, invalid) revealed a main effect of Validity, $F(1, 22) = 5.1$, $p = .034$, $\eta_p^2 = .189$) with higher accuracy in valid trials. The factor Prior and the interaction did not reach significance.

The within-participant ANOVA on mean RT in each condition with the factors Prior (true, false), Block (90% CV, 70%CV, 30%CV, 10%CV), and Validity (valid, invalid) revealed a main effect of Prior ($F(1, 22) = 7.8$, $p = .011$, $\eta_p^2 = .261$), with higher RTs in false blocks, a main effect of Validity ($F(1, 22) = 20.9$, $p = 1.5 \times 10^{-4}$, $\eta_p^2 = .487$), with higher RTs in invalid trials, as well as a significant Prior × Block × Validity interaction ($F(1.46, 32.04) = 22.7$, $p = 3 \times 10^{-10}$, $\eta_p^2 = .508$). To further interpret the interaction, we subjected the difference in RTs between invalid and valid trials, that is, the VE, to a 2 × 2 within-participant ANOVA with the factors Prior (true, false) and Block (90%CV, 70%CV, 30%CV, 10%CV). The linear trend for the Prior × Block interaction was significant ($F(1, 22) = 33.3$, $p = 8 \times 10^{-6}$, $\eta_p^2 = .602$). As expected, VEs varied linearly with CV%, and this effect had a reversed direction in false blocks reflecting learning of the actual %CV (see Figure 1B). This confirms that the participants inferred the actual %CV levels in the present paradigm.

Regarding belief updating, we compared the learning rate α of the RW learning model between blocks with true and false priors using a paired-samples t test. As hypothesized,

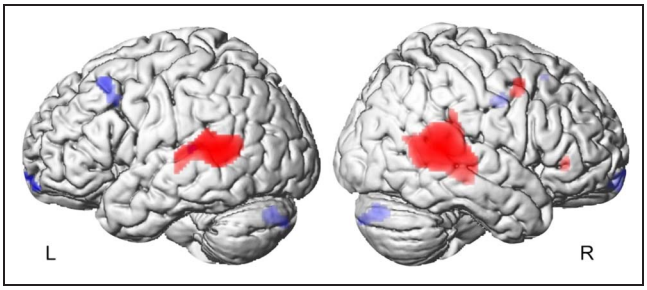

Figure 2. Positive (red) and negative (blue) rsFC of rTPJ across both resting-state runs.

this revealed a significant difference ($t(22) = -2.7$, $p = .012$), with a higher learning rate in blocks with false priors, that is, when more belief updating was required.

Because the study was performed on multiple days, we additionally tested with dedicated two-sample t tests whether there were any session effects for the mean VE or the belief updating parameter (i.e., the difference between true and false blocks of the learning rate α). These analyses did not reveal any significant session order effects (VE: $t(21) = 0.38$, $p = .708$; learning rate difference: $t(21) = -0.993$, $p = .332$).

We also checked if the mean VE and the difference score of the learning rate α were correlated. The correlation between both measures was not significant ($r = -.235$, $p = .28$).

rsFC of rTPJ

Seed-based analysis of rsFC of the specific rTPJ coordinate across pre- and posttask runs revealed significant positive rsFC with bilateral TPJ, rIFG, and right FEF. Significant negative rsFC of the rTPJ was found with the left superior frontal gyrus, the left superior orbital gyrus, and the cerebellum (Figure 2; see Table 1 for full list).

The comparison between pre- and posttask runs did not reveal any significant results. As for behavioral data, there were also no significant session order effects.

Linking rTPJ Functional Connectivity and Behavior

Reorienting of Attention

ROI-based correlation analyses between behavior and rsFC of rTPJ were performed with six predefined ROIs, with coordinates derived from the local maxima in the respective anatomical region from the rsFC maps of rTPJ across both resting-state runs (lTPJ: $x = -62$, $y = -52$, $z = 14$; rIFG: $x = 42$, $y = 12$, $z = 12$; lFEF: $x = -56$, $y = -2$, $z = 48$; rFEF: $x = 42$, $y = 2$, $z = 46$; lIPS: $x = -26$, $y = -72$, $z = 42$; rIPS: $x = 26$, $y = -72$, $z = 56$). Pretask rsFC of rTPJ was not significantly related to the general speed of reorienting, that is, to the overall magnitude of the VE. However, the VE was negatively correlated with the change in rsFC between rTPJ and lTPJ from pre- to posttask ($r = -.59$, $p = .003$; Figure 3). Stronger interhemispheric rsFC between lTPJ and rTPJ after (as compared with before) the task was associated with a smaller overall VE. The analysis of Cook's distance revealed one outlier (>1). However, the correlation remained significant when excluding this outlier ($r = -.44$, $p = .042$). A stepwise linear regression revealed that besides the VE, the belief updating parameter also contributed to the explanation of the rsFC changes between rTPJ and lTPJ (AICC = −86.52 for both predictor variables vs. AICC = −85.26 for VE as the only predictor variable).

Table 1. rsFC Pattern of the rTPJ across Both Resting-state Runs

				Peak Voxel (MNI Coordinates)		
Region	*Cluster Size*	*Side*	*t*	*x*	*y*	*z*
Positive functional connectivity						
Superior/middle temporal gyrus (TPJ)	2457	R	39.07	60	−44	12
Superior/middle temporal gyrus (TPJ)	1080	L	14.24	−62	−52	14
IFG	20	R	8.43	40	30	4
Precentral gyrus (FEF)	45	R	8.08	42	2	46
Negative functional connectivity						
Superior frontal gyrus	82	L	9.59	−22	16	52
Middle cingulate gyrus/white matter	20	R	8.62	18	−8	40
Posterior cingulate gyrus/white matter	29	L	8.53	−4	−34	12
Superior/middle orbital gyrus	40	L	8.12	−26	60	−12
Cerebellum	92	R	7.82	4	−82	−26

R = right; L = left.

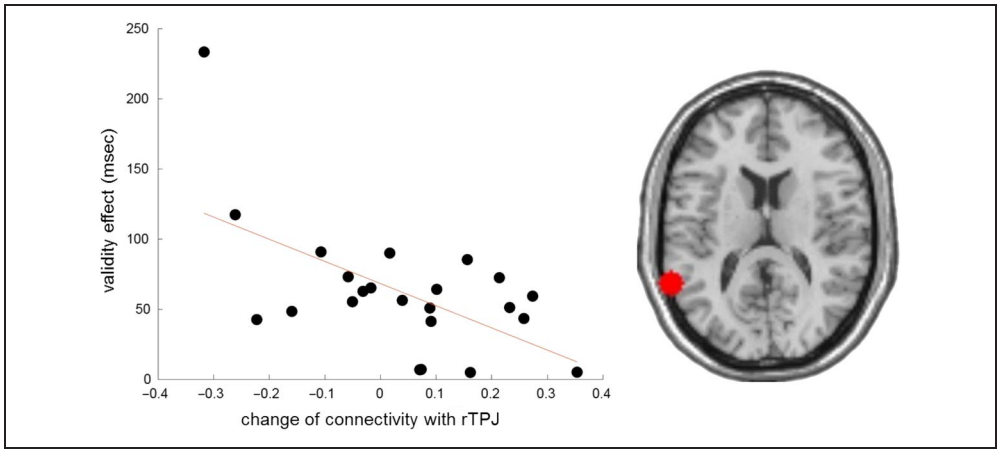

Figure 3. Correlation of the parameter of reorienting (mean VE) and the change in rsFC between the rTPJ and the lTPJ after (as compared with before) the task.

Belief Updating

For the association between behavior and pretask rsFC, we found a significant negative correlation between belief updating (as reflected in the difference in learning rates for false and true blocks) and the strength of rsFC between the rTPJ and rIPS ($r = -.44$, $p = .037$; Figure 4). Here, stronger rsFC between rTPJ and rIPS before the task was related to reduced updating (i.e., a smaller difference in learning rates). According to a stepwise linear regression, the belief updating parameter was the only relevant predictor variable (i.e., the VE was eliminated from the regression model) for rTPJ–rIPS connectivity. All of Cook's distance values were below 1. Regarding rTPJ rsFC after (as compared with before) the task, a significant positive correlation between updating and the change of rsFC between the rTPJ and lTPJ from pre- to posttask was observed ($r = .43$, $p = .043$; Figure 4). Faster updating (in false vs. true blocks) was associated with stronger interhemispheric rsFC between lTPJ and rTPJ after (as compared with before) the task. This result is in line with the stepwise regression described above, according to which both belief updating and reorienting contributed to the change in rsFC.

Control Analyses

Additional correlation analyses were performed between the rsFC of rTPJ and more general behavioral

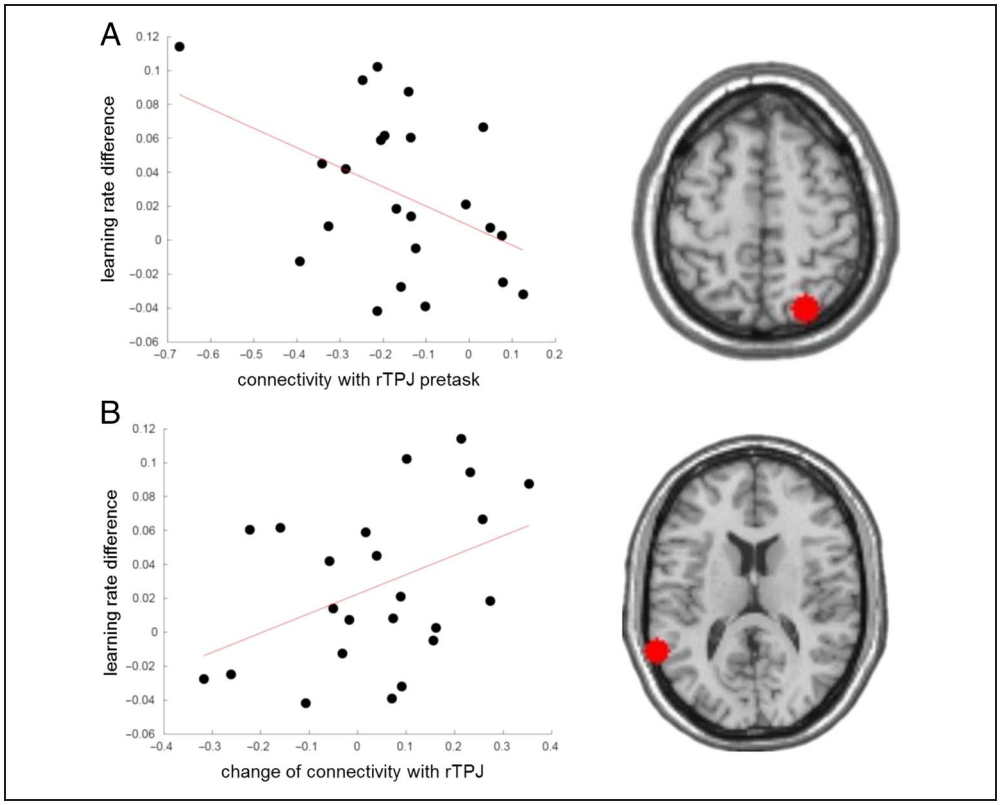

Figure 4. Correlations of belief updating and the rsFC between the rTPJ and the rIPS before the task as well as between the rTPJ and lTPJ after (as compared with before) the task.

parameters, that is, overall RS and accuracy. In none of the six ROIs, these analyses revealed significant effects (all $ps > .05$).

DISCUSSION

This study investigated whether the resting-state network architecture of rTPJ with ventral and dorsal attention network nodes is related to belief updating and reorienting. In a modified location-cueing paradigm, blockwise changes of the %CV were implemented, and true and false prior information about the %CV was provided before each block. Higher functional connectivity between rTPJ and rIPS before the task was associated with a smaller difference in learning rates between false and true blocks, that is, with slower belief updating after false priors. Increases in connectivity between rTPJ and lTPJ after the task were related to both relatively faster belief updating in false blocks and faster reorienting (smaller VEs).

Regarding the behavioral results, we replicated previous findings with the same experimental paradigm (Mengotti et al., 2017). As expected, VEs varied linearly with %CV, and this effect had a reversed direction in false blocks, reflecting learning of the actual %CV. Moreover, participants had a higher learning rate in blocks with false as compared with true prior information (when belief updating was required).

Our results regarding the rsFC pattern of the specific rTPJ coordinate are consistent with previous studies on rsFC of rTPJ (Bzdok et al., 2013; Kucyi et al., 2012; Mars et al., 2012; Shulman et al., 2009), showing positive connectivity between rTPJ and other regions of the ventral attention network, that is, rIFG. Our positive rsFC pattern especially relates to findings of the rsFC of an anterior cluster of the rTPJ, which has been associated with attentional functions in task-based studies (Bzdok et al., 2013). Furthermore, our findings on the negative rsFC are in line with previous work reporting negative connectivity of rTPJ with frontal regions and the cerebellum, although not all previously described regions showed significant results in this study (Kucyi et al., 2012).

Investigating the association between the rsFC of the rTPJ and the behavioral parameters from the location-cueing paradigm revealed specific relationships for belief updating and reorienting, respectively. As a note of caution, these findings were derived from a correlational approach and thus cannot be interpreted as causal effects. General behavioral parameters such as mean RS and accuracy were not significantly related to the rsFC patterns of rTPJ. Faster belief updating in false versus true blocks was associated with weaker rsFC of rTPJ with rIPS before the task. IPS is regarded as a key region of the dorsal system responsible for top–down control and selection (Corbetta, Kincade, Ollinger, McAvoy, & Shulman, 2000; Hopfinger, Buonocore, & Mangun, 2000; Kastner, Pinsk, De Weerd, Desimone, & Ungerleider, 1999). Hence, the intrahemispheric rIPS–rTPJ connection may reflect the strength of the reliance on top–down information, that is, in our case, the a priori %CV. Firm reliance on this prior information may then lead to slower updating of %CV, that is, to a smaller influence of prediction errors on the trial-wise estimation of the probability that the cue will be valid (as parameterized in the learning rate parameter of the RW model). In line with this notion, first evidence exists for an involvement of IPS in contextual updating in a sustained attention task. Here, TMS over IPS suppressed TPJ responses for differentiating targets and nontargets, suggesting that IPS gives input to TPJ to shape stimulus-evoked responses (Leitão, Thielscher, Tunnerhoff, & Noppeney, 2015).

Regression analysis revealed that rsFC between rTPJ and rIPS was related to belief updating rather than reorienting. This may seem at odds with previous studies showing an involvement of IPS in reorienting of spatial attention (Vossel et al., 2012; Weissman & Prado, 2012; Wen et al., 2012; Chica, Bartolomeo, & Valero-Cabre, 2011). However, our present results concern the state of the network architecture before the task, rather than connectivity during the task. Hence, the IPS—or connectivity between rTPJ and IPS (see Vossel et al., 2012)—may still play an essential role in online task performance. This, together with the network effects of rTPJ neurostimulation, will be addressed in our future work.

When investigating the interhemispheric connectivity between rTPJ and lTPJ, we found that better behavior (relatively faster updating in false blocks and faster reorienting) was accompanied by an increase in the rsFC between the rTPJ and the lTPJ after (as compared with before) the task. Regression analysis revealed that both reorienting and belief updating contributed to the explanation of interhemispheric rsFC changes between rTPJ and lTPJ. It has been suggested that both lTPJ and rTPJ are vital for updating the statistical contingency between cues and targets, with rTPJ coding mismatches between cues and targets and lTPJ coding with cue–target matches (Doricchi et al., 2010). Moreover, previous task-based fMRI studies on other attentional functions have shown that effective connectivity between lTPJ and rTPJ is related to enhanced filtering of distractors in a partial report paradigm (Vossel et al., 2016). Our results also support and extend findings from patient studies that interhemispheric parietal and temporoparietal interactions are essential for attentional functions (Siegel et al., 2016; Baldassarre et al., 2014; Carter et al., 2010; He et al., 2007). These studies emphasize that a decrease in interhemispheric rsFC, presumably due to an imbalance between both hemispheres after stroke, is related to impaired performance in a location-cueing task and cancellation tests.

Besides, patient studies investigating the effects of non-invasive brain stimulation over parietal cortex for the recovery of neglect symptoms after stroke showed that stimulation protocols could improve impaired behavior (see Salazar et al., 2018, for a review). For instance, both

cathodal direct current stimulation of the unlesioned posterior parietal cortex and anodal stimulation of the lesioned homologous region reduced symptoms of neglect (Sparing et al., 2009). Furthermore, inhibitory TMS on the contralesional left parietal cortex likewise ameliorated neglect (Nyffeler et al., 2019). However, the response rate to the stimulation depended on the integrity of the interhemispheric connections, especially of the corpus callosum connecting homologous parietal regions (Nyffeler et al., 2019). This is in line with findings of healthy participants, where the structural variability within the corpus callosum was a predictor for the individual differences in the effects of inhibitory TMS on the posterior parietal cortex on the allocation of spatial attention (Chechlacz, Humphreys, Sotiropoulos, Kennard, & Cazzoli, 2015). Consequently, an amelioration of the interhemispheric rsFC between the posterior parietal cortices was found to be associated with the recovery of neglect symptoms (Ramsey et al., 2016), which again emphasizes the importance of intact interhemispheric rsFC for cognitive functions. Here, we show that this is not only relevant for attentional functions, but also the updating of probabilistic beliefs.

However, our present results not only suggest that resting-state connectivity per se is relevant for cognitive functions but also that cognitive processing during a task can change connectivity patterns afterwards in a performance-dependent manner. It has been proposed that the rsFC pattern of a person may be seen as a trait that can be used to predict behavior and disease (Khosla, Jamison, Ngo, Kuceyeski, & Sabuncu, 2019; Craddock, Holtzheimer, Hu, & Mayberg, 2009). Although our findings are in accord with this notion, they also suggest that the relationship between rsFC and behavior may be more complex, with mutual interactions between cognitive processing and resting-state connectivity architectures.

Conclusions

We have provided resting-state fMRI evidence that rsFC before task and changes in rsFC from pre- to posttask of the rTPJ are related to belief updating and reorienting in a Posner task with uncertain contingencies between cues and targets. Therefore, this study highlights the mutual influence of functional connectivity during rest and behavior. Moreover, it identifies IPS as a crucial network node for rTPJ for the flexible deployment of attention in relation to inferred cue validity.

Acknowledgments

This work was supported by funding from the Federal Ministry of Education and Research to S. V. (BMBF, 01GQ1401). We are grateful to our colleagues from the INM-3 and INM-4 for valuable support and discussions.

Reprint requests should be sent to Anne-Sophie Käsbauer, Cognitive Neuroscience, Institute of Neuroscience and Medicine (INM-3), Research Centre Juelich, Leo-Brandt-Str. 5, 52425 Juelich, Germany, or via e-mail: a.kaesbauer@fz-juelich.de.

REFERENCES

Baldassarre, A., Ramsey, L., Hacker, C. L., Callejas, A., Astafiev, S. V., Metcalf, N. V., et al. (2014). Large-scale changes in network interactions as a physiological signature of spatial neglect. *Brain*, *137*, 3267–3283.

Behzadi, Y., Restom, K., Liau, J., & Liu, T. T. (2007). A component based noise correction method (CompCor) for BOLD and perfusion based fMRI. *Neuroimage*, *37*, 90–101.

Biswal, B., Yetkin, F. Z., Haughton, V. M., & Hyde, J. S. (1995). Functional connectivity in the motor cortex of resting. *Magnetic Resonance in Medicine*, *34*, 537–541.

Brodersen, K. H., Penny, W. D., Harrison, L. M., Daunizeau, J., Ruff, C. C., Duzel, E., et al. (2008). Integrated Bayesian models of learning and decision making for saccadic eye movements. *Neural Networks*, *21*, 1247–1260.

Bzdok, D., Langner, R., Schilbach, L., Jakobs, O., Roski, C., Caspers, S., et al. (2013). Characterization of the temporo-parietal junction by combining data-driven parcellation, complementary connectivity analyses, and functional decoding. *Neuroimage*, *81*, 381–392.

Carpenter, R. H., & Williams, M. L. (1995). Neural computation of log likelihood in control of saccadic eye movements. *Nature*, *377*, 59–62.

Carter, A. R., Astafiev, S. V., Lang, C. E., Connor, L. T., Rengachary, J., Strube, M. J., et al. (2010). Resting interhemispheric functional magnetic resonance imaging connectivity predicts performance after stroke. *Annals of Neurology*, *67*, 365–375.

Chechlacz, M., Humphreys, G. W., Sotiropoulos, S. N., Kennard, C., & Cazzoli, D. (2015). Structural organization of the corpus callosum predicts attentional shifts after continuous theta burst stimulation. *Journal of Neuroscience*, *35*, 15353–15368.

Chica, A. B., Bartolomeo, P., & Valero-Cabre, A. (2011). Dorsal and ventral parietal contributions to spatial orienting in the human brain. *Journal of Neuroscience*, *31*, 8143–8149.

Cook, R. D. (1977). Detection of influential observation linear regression. *Technometrics*, *19*, 15–18.

Corbetta, M., Kincade, J. M., Ollinger, J. M., McAvoy, M. P., & Shulman, G. L. (2000). Voluntary orienting is dissociated from target detection in human posterior parietal cortex. *Nature Neuroscience*, *3*, 292–297.

Corbetta, M., Patel, G., & Shulman, G. L. (2008). The reorienting system of the human brain: From environment to theory of mind. *Neuron*, *58*, 306–324.

Corbetta, M., Ramsey, L., Callejas, A., Baldassarre, A., Hacker, C. D., Siegel, J. S., et al. (2015). Common behavioral clusters and subcortical anatomy in stroke. *Neuron*, *85*, 927–941.

Corbetta, M., & Shulman, G. L. (2002). Control of goal-directed and stimulus-driven attention in the brain. *Nature Reviews Neuroscience*, *3*, 201–215.

Craddock, R. C., Holtzheimer, P. E., III, Hu, X. P., & Mayberg, H. S. (2009). Disease state prediction from resting state functional connectivity. *Magnetic Resonance in Medicine*, *62*, 1619–1628.

Daunizeau, J., den Ouden, H. E. M., Pessiglione, M., Kiebel, S. J., Friston, K. J., & Stephan, K. E. (2010). Observing the

observer (II): Deciding when to decide. *PLoS One*, *5*, e15555.
Doricchi, F., Macci, E., Silvetti, M., & Macaluso, E. (2010). Neural correlates of the spatial and expectancy components of endogenous and stimulus-driven orienting of attention in the posner task. *Cerebral Cortex*, *20*, 1574–1585.
Eickhoff, S. B., Stephan, K. E., Mohlberg, H., Grefkes, C., Fink, G. R., Amunts, K., et al. (2005). A new SPM toolbox for combining probabilistic cytoarchitectonic maps and functional imaging data. *Neuroimage*, *25*, 1325–1335.
Fox, M. D., Corbetta, M., Snyder, A. Z., Vincent, J. L., & Raichle, M. E. (2006). Spontaneous neuronal activity distinguishes human dorsal and ventral attention systems. *Proceedings of the National Academy of Sciences, U.S.A.*, *103*, 10046–10051.
Fox, M. D., Snyder, A. Z., Vincent, J. L., Corbetta, M., Van Essen, D. C., & Raichle, M. E. (2005). From the cover: The human brain is intrinsically organized into dynamic, anticorrelated functional networks. *Proceedings of the National Academy of Sciences, U.S.A.*, *102*, 9673–9678.
Friston, K. J., Holmes, A. P., Worsley, K. J., Poline, J.-P., Frith, C. D., & Frackowiak, R. S. J. (1995). Statistical parametric maps in functional imaging: A general linear approach. *Human Brain Mapping*, *2*, 189–210.
Friston, K., Mattout, J., Trujillo-Barreto, N., Ashburner, J., & Penny, W. (2007). Variational free energy and the laplace approximation. *Neuroimage*, *34*, 220–234.
Geng, J. J., & Vossel, S. (2013). Re-evaluating the role of TPJ in attentional control: Contextual updating? *Neuroscience and Biobehavioral Reviews*, *37*, 2608–2620.
Greicius, M. D., Supekar, K., Menon, V., & Dougherty, R. F. (2009). Resting-state functional connectivity reflects structural connectivity in the default mode network. *Cerebral Cortex*, *19*, 72–78.
He, B. J., Snyder, A. Z., Vincent, J. L., Epstein, A., Shulman, G. L., & Corbetta, M. (2007). Breakdown of functional connectivity in frontoparietal networks underlies behavioral deficits in spatial neglect. *Neuron*, *53*, 905–918.
Hoffstaedter, F., Grefkes, C., Caspers, S., Roski, C., Palomero-Gallagher, N., Laird, A. R., et al. (2014). The role of anterior midcingulate cortex in cognitive motor control. *Human Brain Mapping*, *35*, 2741–2753.
Honey, C. J., Sporns, O., Cammoun, L., Gigandet, X., Thiran, J. P., Meuli, R., et al. (2009). Predicting human resting-state functional connectivity. *Proceedings of the National Academy of Sciences, U.S.A.*, *106*, 2035–2040.
Hopfinger, J. B., Buonocore, M. H., & Mangun, G. R. (2000). The neural mechanisms of attentional control. *Nature Neuroscience*, *3*, 284–291.
Igelström, K. M., & Graziano, M. S. A. (2017). The inferior parietal lobule and temporoparietal junction: A network perspective. *Neuropsychologia*, *105*, 70–83.
Iglesias, S., Mathys, C., Brodersen, K. H., Kasper, L., Piccirelli, M., denOuden, H. E., et al. (2013). Hierarchical prediction errors in midbrain and basal forebrain during sensory learning. *Neuron*, *80*, 519–530.
Kastner, S., Pinsk, M. A., De Weerd, P., Desimone, R., & Ungerleider, L. G. (1999). Increased activity in human visual cortex during directed attention in the absence of visual stimulation. *Neuron*, *22*, 751–761.
Khosla, M., Jamison, K., Ngo, G. H., Kuceyeski, A., & Sabuncu, M. R. (2019). Machine learning in resting-state fMRI analysis. *Magnetic Resonance Imaging*, *64*, 101–121.
Krall, S. C., Volz, L. J., Oberwelland, E., Grefkes, C., Fink, G. R., & Konrad, K. (2016). The right temporoparietal junction in attention and social interaction: A transcranial magnetic stimulation study. *Human Brain Mapping*, *37*, 796–807.
Kucyi, A., Hodaie, M., & Davis, K. D. (2012). Lateralization in intrinsic functional connectivity of the temporoparietal junction with salience- and attention-related brain networks. *Journal of Neurophysiology*, *108*, 3382–3392.
Leitão, J., Thielscher, A., Tunnerhoff, J., & Noppeney, U. (2015). Concurrent TMS-fMRI reveals interactions between dorsal and ventral attentional systems. *Journal of Neuroscience*, *35*, 11445–11457.
Mars, R. B., Sallet, J., Schüffelgen, U., Jbabdi, S., Toni, I., & Rushworth, M. F. (2012). Connectivity-based subdivisions of the human right "temporoparietal junction area": Evidence for different areas participating in different cortical networks. *Cerebral Cortex*, *22*, 1894–1903.
Mengotti, P., Dombert, P. L., Fink, G. R., & Vossel, S. (2017). Disruption of the right temporoparietal junction impairs probabilistic belief updating. *Journal of Neuroscience*, *37*, 5419–5428.
Nyffeler, T., Vanbellingen, T., Kaufmann, B. C., Pflugshaupt, T., Bauer, D., Frey, J., et al. (2019). Theta burst stimulation in neglect after stroke: Functional outcome and response variability origins. *Brain*, *142*, 992–1008.
Oldfield, R. C. (1971). The assessment and analysis of handedness: The Edinburgh inventory. *Neuropsychologia*, *9*, 97–113.
Posner, M. I. (1980). Orienting of attention. *Quarterly Journal of Experimental Psychology*, *32*, 3–25.
Ramsey, L. E., Siegel, J. S., Baldassarre, A., Metcalf, N. V., Zinn, K., Shulman, G. L., et al. (2016). Normalization of network connectivity in hemispatial neglect recovery. *Annals of Neurology*, *80*, 127–141.
Rushworth, M. F. S., & Behrens, T. E. J. (2008). Choice, uncertainty and value in prefrontal and cingulate cortex. *Nature Neuroscience*, *11*, 389–397.
Salazar, A. P. S., Vaz, P. G., Marchese, R. R., Stein, C., Pinto, C., & Pagnussat, A. S. (2018). Noninvasive brain stimulation improves hemispatial neglect after stroke: A systematic review and meta-analysis. *Archives of Physical Medicine and Rehabilitation*, *99*, 355–366.
Shulman, G. L., Astafiev, S. V., Franke, D., Pope, D. L., Snyder, A. Z., McAvoy, M. P., et al. (2009). Interaction of stimulus-driven reorienting and expectation in ventral and dorsal frontoparietal and basal ganglia-cortical networks. *Journal of Neuroscience*, *29*, 4392–4407.
Siegel, J. S., Ramsey, L. E., Snyder, A. Z., Metcalf, N. V., Chacko, R. V., Weinberger, K., et al. (2016). Disruptions of network connectivity predict impairment in multiple behavioral domains after stroke. *Proceedings of the National Academy of Sciences, U.S.A.*, *113*, 4367–4376.
Silvetti, M., Lasaponara, S., Lecce, F., Dragone, A., Macaluso, E., & Doricchi, F. (2016). The response of the left ventral attentional system to invalid targets and its implication for the spatial neglect syndrome: A multivariate fMRI investigation. *Cerebral Cortex*, *26*, 4551–4562.
Sparing, R., Thimm, M., Hesse, M. D., Küst, J., Karbe, H., & Fink, G. R. (2009). Bidirectional alterations of interhemispheric parietal balance by non-invasive cortical stimulation. *Brain*, *132*, 3011–3020.
Stevens, J. (1996). *Applied multivariate statistics for the social sciences* (6th ed.). Mahwah, NJ: Erlbaum.
Vossel, S., Mathys, C., Daunizeau, J., Bauer, M., Driver, J., Friston, K. J., et al. (2014). Spatial attention, precision, and bayesian inference: A study of saccadic response speed. *Cerebral Cortex*, *24*, 1436–1450.
Vossel, S., Mathys, C., Stephan, K. E., & Friston, K. J. (2015). Cortical coupling reflects bayesian belief updating in the deployment of spatial attention. *Journal of Neuroscience*, *35*, 11532–11542.
Vossel, S., Weidner, R., Driver, J., Friston, K. J., & Fink, G. R. (2012). Deconstructing the architecture of dorsal and ventral

attention systems with dynamic causal modeling. *Journal of Neuroscience*, *32*, 10637–10648.
Vossel, S., Weidner, R., Moos, K., & Fink, G. R. (2016). Individual attentional selection capacities are reflected in interhemispheric connectivity of the parietal cortex. *Neuroimage*, *129*, 148–158.
Weissman, D. H., & Prado, J. (2012). Heightened activity in a key region of the ventral attention network is linked to reduced activity in a key region of the dorsal attention network during unexpected shifts of covert visual spatial attention. *Neuroimage*, *61*, 798–804.
Wen, X., Yao, L., Liu, Y., & Ding, M. (2012). Causal interactions in attention networks predict behavioral performance. *Journal of Neuroscience*, *32*, 1284–1292.
Whitfield-Gabrieli, S., & Nieto-Castanon, A. (2012). Conn: A functional connectivity toolbox for correlated and anticorrelated brain networks. *Brain Connectivity*, *2*, 125–141.
Yeo, B. T., Krienen, F. M., Sepulcre, J., Sabuncu, M. R., Lashkari, D., Hollinshead, M., et al. (2011). The organization of the human cerebral cortex estimated by intrinsic functional connectivity. *Journal of Neurophysiology*, *106*, 1125–1165.